JACS
JOURNAL OF THE AMERICAN CHEMICAL SOCIETY
Article
pubs.acs.org/JACS

Molecular Stirrers in Action

Jiawen Chen, Jos C. M. Kistemaker, Jort Robertus, and Ben L. Feringa*

Centre for Systems Chemistry, Stratingh Institute for Chemistry and Zernike Institute for Advanced Materials, University of Groningen, Nijenborgh 4, 9747 AG Groningen, The Netherlands

Web-Enhanced Feature *Supporting Information*

ABSTRACT: A series of first-generation light-driven molecular motors with rigid substituents of varying length was synthesized to act as "molecular stirrers". Their rotary motion was studied by ^{1}H NMR and UV−vis absorption spectroscopy in a variety of solvents with different polarity and viscosity. Quantitative analyses of kinetic and thermodynamic parameters show that the rotary speed is affected by the rigidity of the substituents and the length of the rigid substituents and that the differences in speed are governed by entropy effects. Most pronounced is the effect of solvent viscosity on the rotary motion when long, rigid substituents are present. The α values obtained by the *free volume* model, supported by DFT calculations, demonstrate that during the rotary process of the motor, as the rigid substituent becomes longer, an increased rearranging volume is needed, which leads to enhanced solvent displacement and retardation of the motor.

1. INTRODUCTION

Molecular motors are abundant in nature, driving a variety of essential biological processes.[1] These ingenious systems are a great source of inspiration and set the stage for a long-standing goal in current nanotechnology toward the design and exploration of molecular systems that govern controlled rotary and translational motion and ultimately make it possible to operate more complex machine-like functions.[2] In studying the dynamics of motors in solution at the nanoscale, under conditions of low Reynolds numbers[3] and where Brownian motion rules, it should be remembered that non-covalent interactions are key, in contrast to the functioning of macroscopic motors, where inertia is a dominant factor.[4] A recurrent question is to what extent molecular size and rigidity and the effects of the nanoscale environment—i.e., solvent polarity and viscosity and surface friction—play roles in governing rotary motion.

Control over rotary and translational motion with molecular systems has been achieved in the past decade with a variety of rotors,[5] motors,[6] shuttles,[7] propulsion systems,[8] and walkers,[9] both in solution and on surfaces,[10] and these systems are powered by light, heat, redox processes, or chemical conversions. Our program on molecular motors focuses on light-driven unidirectional rotary motors based on chiral, overcrowded alkenes.[11]

The first-generation motor[12] consists of two identical chromophores linked by an olefinic bond (Figure 1). The central carbon−carbon double bond acts as the axle for rotation, and the rotary motion is induced by photochemical stilbene-type photoisomerization. Repetitive rotation around the double bond is achieved by two energetically uphill photochemical steps, each followed by a thermally activated, energetically downhill step. The chirality of the molecular motor allows the rotation to proceed in a unidirectional sense. The combination of being able to rotate repetitively with controlled directionality,[13] powered by light energy, qualifies the system as a rotary molecular motor and distinguishes the motor from many systems based on molecular switches.[14] In addition, the large geometrical change of the two halves of the first-generation motor with respect to each other upon isomerization can be used for stereodynamic control in mesoscopic and macromolecular materials[15] and for precise positioning of functional groups in a dynamic cycle with sequence control. This resulted in a variety of applications, including dynamic control of intramolecular H-stacking of perylenebisimide,[16] controlling intramolecular through-space magnetic interactions,[17] functioning as molecular "gear box",[18] and photoswitchable chiral organocatalysts.[19] The geometrical change that the motor undergoes during its rotary process might be able to displace the surrounding solvent molecules,[20] and the large-amplitude motion is expected to be affected by solvent friction. It has indeed been demonstrated that isomerization processes that involve large-amplitude rotational motion are controlled by the viscosity of the medium, although the effects are in some cases remarkably small.[21f,g] External frictional effects have been observed in viscous solvents and compressed liquids for photochemical and thermal isomerizations of stilbenes[22] and azobenzenes,[23] rearrangements and fragmentations,[24] local rotations in peptides and proteins,[25] *E*−

Figure 1. Molecular stirrer based on a first-generation light-driven molecular motor.

Received: July 29, 2014
Published: September 25, 2014

ACS Publications © 2014 American Chemical Society

dx.doi.org/10.1021/ja507711h | *J. Am. Chem. Soc.* 2014, 136, 14924−14932

Scheme 1. First-Generation Light-Driven Molecular Motors 1−5 with Different Rods at the 6- and 6′-Positions

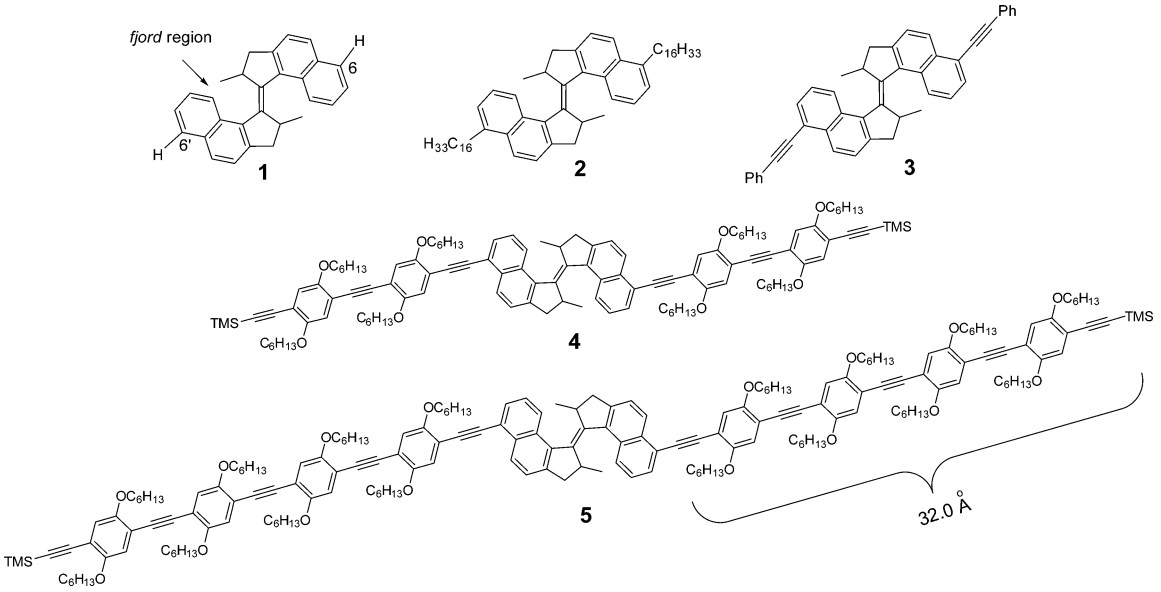

Z isomerization in photochromic dendrimers,[21g] and rotary motion of surface-bound rotors.[26] A pertinent example of an azobenzene derivative acting as a "molecular stirrer" was reported by Tanaka,[27] resulting in the controlled release of a guest from a zeolite pore. The influence of substituents on the photoisomerization of dendrimer-based azobenzenes has been discussed by Müllen and De Schryver,[28] showing that the rigidity and the size of the rigid dendritic wedges have a modest (factor of 3) but significant effect on the rate constant of the thermal *cis*−*trans* isomerization in higher generation dendrimers with an azobenzene core. Other examples include isomerization of 1,4-diphenyl-1,3-butadiene,[29] merocyanine,[30] bisoxonols,[31] carbocyanine,[32] and zinc dithizonate.[33] Adam and Trofimov emphasized that solvent viscosity studies and analyses in terms of a free-volume model provide important insight into frictional effects in molecular transformations.[34] We considered it of great interest to explore whether an extension of the rotary motor with longer "arms" would experience greater frictional effects and enable it to displace more solvent, with the ultimate goal of applying these systems as light-powered molecular stirrers (Figure 1). Therefore, exploring the properties of molecular motors with substituents of distinct size, length, and rigidity in an environment of increasing viscosity could help us gain more insight in the rotary process of molecular motors.

In the present study, two main questions were investigated. First, what is the effect of covalently bound large and/or rigid groups on the rotary motion of the light-driven motor? Second, what is the effect on the speed of a motor when it rotates in a viscous solvent compared to a non-viscous solvent? In the nanoscale world, the possibility exists that a molecular motor would rotate inside its solvent shell and therefore not be affected by the size of substituents and the viscosity of the surrounding solvent. Increasing the length of the motor's substituents might result in a protrusion of the solvent shell which would allow the viscosity of the surrounding solvent to affect the rotary motion. We anticipated that a rod-like substituent will require a different degree of order of the surroundings than a flexible chain, and we expected that it might display a higher entropic barrier.

2. RESULTS AND DISCUSSION

2.1. Design. The molecular stirrers in the present study are based on first-generation molecular motors with two pending rods (Scheme 1). In the design of light-driven motors with rods of various lengths and flexibility, it is essential that the pending rods do not interfere with the rotary behavior (Scheme 1). DFT calculations suggest that substituents placed at the 6- and 6′-positions of the naphthalene ring of first-generation motor **1** (Scheme 1) do not exert a direct effect on the steric crowding in the *fjord* region, as shown by the insignificant differences found for the enthalpies of activation (Supporting Information (SI), Table S3). In addition, as reported previously,[35] electronic effects caused by substitution at this position do not have a significant influence on the rotary speed of the motor. Therefore, a series of molecular motors was designed with different substituents, including long, flexible hexadecyl chains and rigid phenylethynylene oligomers with varying lengths which have been introduced on both sides of the motor core structure (Scheme 1). Phenylethynylene oligomers were chosen because they are known to be shape persistent and their synthesis allows for well-defined sizes of the rods.[36] With this design, we envisioned good control over the length of the rigid oligomers attached to the motors. In the molecules **1**−**5** (Scheme 1), the length of the rods varied from H (1.09 Å) to tetramer (32.0 Å). The rotary motion of these motors was studied by ^{1}H NMR and UV−vis spectroscopy using solvents with different polarities and viscosities.

2.2. Synthesis. The synthesis of molecular motors **1**−**5** involves dibromo-substituted, overcrowded alkene **9** as a key intermediate for subsequent coupling reactions of various rods. For the regioselective synthesis of the 6-bromo ketone **8** (Scheme 2), we started with ketone **6**,[37] which was treated with bromine under Lewis acid conditions at 40 °C, resulting first in the α-brominated intermediate which was not isolated. Upon addition of an excess of bromine, a second bromine substituent was introduced by electrophilic aromatic substitution of the naphthalene moiety with high regioselectivity in favor of the 6-position. After recrystallization from EtOH, dibrominated compound **7** was obtained in moderated yield. Removal of the bromine substituent at the α-position of the ketone was

dx.doi.org/10.1021/ja507711h | J. Am. Chem. Soc. 2014, 136, 14924−14932

Scheme 2. Synthesis of Bis-acetylene-Substituted First-Generation Molecular Motor 11

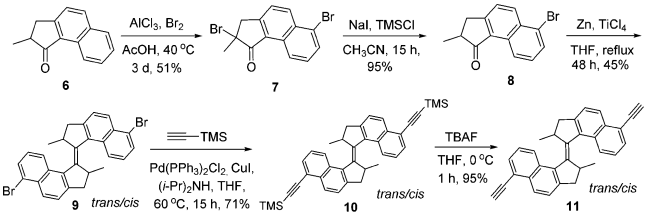

achieved by treating **7** with chlorotrimethylsilane and sodium iodide, giving ketone **8** in nearly quantitative yield . Reductive McMurry coupling of **8** using titanium tetrachloride and zinc provided the overcrowded alkene **9** as a 1:1 mixture of *trans* and *cis* isomers. Further modification was achieved by coupling **9** with trimethylsilylacetylene via Sonagashira coupling, yielding **10** in 71% yield. Deprotection of the trimethylsilyl groups of **10** using tetrabutylammonium fluoride (TBAF) gave rise to motor **11**, which bears two terminal acetylenes that were suitable to be used in a later stage.

For the synthesis of the rigid substituents of varying lengths, building block **12**,[38] which contains two hexyl groups to improve the solubility of the oligomers, was employed. Phenylethynylene oligomers of defined sizes were prepared via a step-by-step synthesis,[36] using Sonogashira cross-coupling methodology (Scheme 3).

Scheme 3. Synthesis of the Rigid Rods of Various Lengths

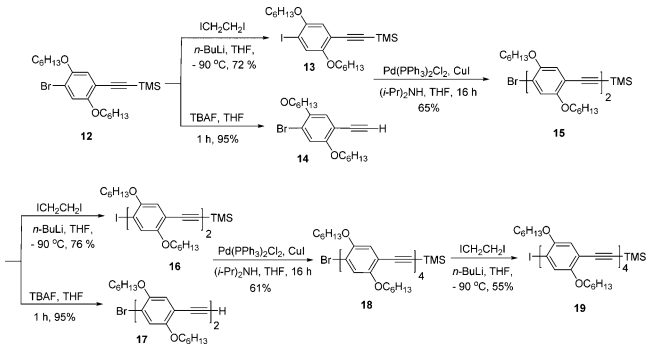

A portion of bromide **12** was converted into the corresponding iodo compound **13**. It is essential to keep the temperature of the reaction mixture strictly below −90 °C to avoid any side reaction. Subsequently, another portion of bromide **12** was treated with TBAF to generate acetylene **14**. Taking advantage of the iodo−bromo selectivity in the Sonagashira cross-coupling, dimer **15** was obtained in 65% yield. No symmetrically coupled oligomers of **14** were observed. This synthetic approach was repeated in an iterative fashion, with the cross-coupling of **16** and **17**, providing tetramer **18** which was further converted into the more reactive aryl iodide **19**.

Subsequently, a variety of cross-coupling methods was employed to connect the light-driven molecular motors with different substituents. For the preparation of **2**, attempts to react dibromo motor **9** with hexadecylboronic acid via Suzuki cross-coupling resulted in a mixture of mono- and disubstituted products which were difficult to separate due to the low polarity of both compounds. Instead, a novel organolithium-based cross-coupling method, recently developed in our group, was applied.[39] Dibromo motor **9** was reacted with hexadecyllithium solution at room temperature in toluene using $Pd[(P^tBu)_3]_2$ as a catalyst (Scheme 4). The reaction was completed within 3 h,

Scheme 4. Coupling of the Motors with Rigid Rods of Various Lengths

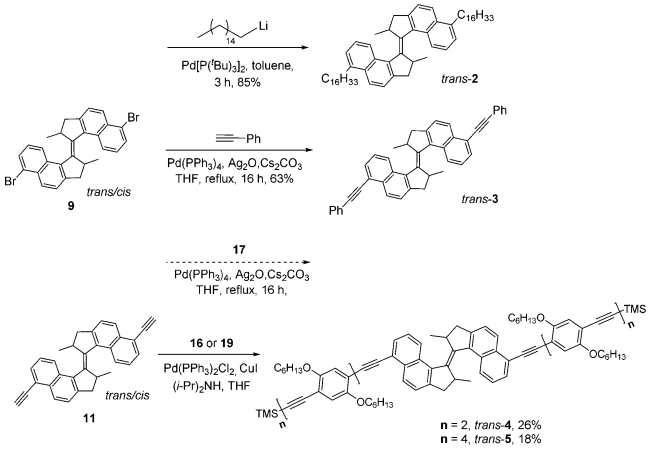

giving 80% yield of the disubstituted product. This coupling method offered in our hands milder conditions, shorter reaction time, higher selectivity, and better yields to install two alkyl groups as in *trans*-**2** than the corresponding Suzuki coupling. The pure *trans* isomer of **2** was obtained by chromatography, and the isomerization processes was studied in accordance with analogues *trans*-**3**−**5** (vide infra).

For the synthesis of **3**, after several reaction conditions were screened, motor **9** was successfully functionalized with phenylacetylene at both the upper and lower halves by using $Pd(PPh_3)_4$, Cs_2CO_3, and Ag_2O as catalysts (Scheme 4). This method prevents homo-coupling of the acetylene compound.[40] After column chromatography, the first-generation molecular motor **3** was isolated as a mixture of *trans* and *cis* isomers in a 10:1 ratio. In contrast, when the same conditions were applied to couple **9** with **17**, no conversion was observed (Scheme 4). Therefore, a reverse coupling approach was used, starting with diacetylene compound **11** (Scheme 4). The cross-coupling between **11** and **16** was performed by using $Pd(Ph_3)_2Cl_2$, CuI, and $(i\text{-Pr})_2NH$, resulting in *trans*-**4**. The low isolated yield (26%) of pure *trans*-**4** is due to poor separation of **4** from various side products by chromatography, while also several recrystallizations were required. Only the monosubstituted *cis* isomer was found; the absence of the disubstituted *cis* isomer of **4** might be due to steric hindrance. Employing the same coupling reaction of **11** with **19**, the pure *trans* isomer of **5** was obtained as the sole disubstituted product in 18% yield. The structures of the isomers were assigned by comparing spectral data with those of various other first-generation motors (for characterization and structural assignment, see the SI).[12]

2.3. ^{1}H NMR Studies. The photoisomerization and thermal helix inversion steps from stable *trans* to stable *cis* isomer of motors **1**−**5** (Scheme 5) were studied by ^{1}H NMR spectroscopy. For first-generation motors, it is expected that, when a stable *trans* isomer with the methyl substituents at the stereogenic center in a pseudoaxial orientation is irradiated with UV light, a photochemical *trans*−*cis* isomerization takes place.[12] This photochemical step results in an unstable *cis* isomer, in which the methyl substituents at the stereogenic centers are forced to adopt a less favored pseudoequatorial

dx.doi.org/10.1021/ja507711h | J. Am. Chem. Soc. 2014, 136, 14924−14932

Scheme 5. Photochemical and Thermal Helix Inversion Steps of 1−5

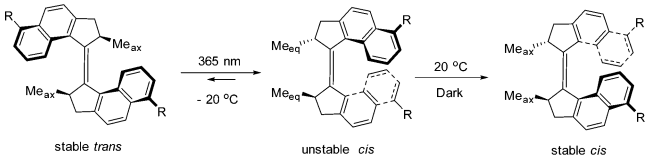

orientation. To release the steric strain, the two naphthalene rings need to slip past each other, resulting in an irreversible thermal isomerization with inverted helical conformation of the molecules. This thermal helix inversion step generates the corresponding stable *cis* isomer, in which the methyl substituents at the stereogenic center adopt a more favored pseudoaxial orientation.

Figure 2a shows the partial ^{1}H NMR spectrum of a solution of stable *trans*-**4** in dichloromethane-d_2 (CD_2Cl_2). (These

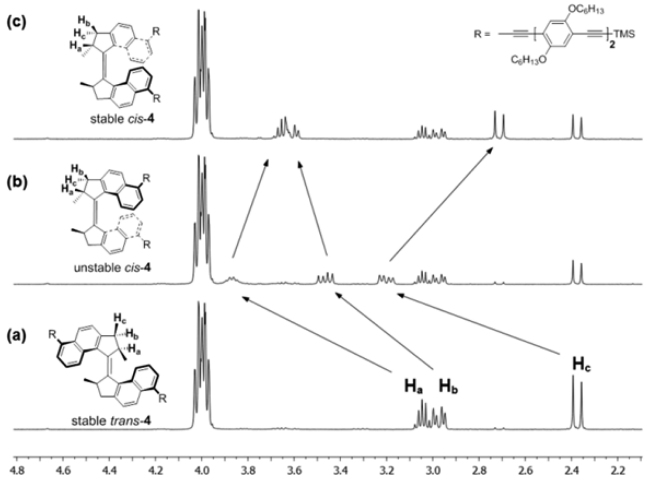

Figure 2. Partial ^{1}H NMR of **4** (CD_2Cl_2, −20 °C): (a) stable *trans*-**4**, before irradiation ($\lambda \geq 365$ nm), (b) after irradiation, and (c) after standing at room temperature in the dark overnight. (Single enantiomer shown.)

spectra are representative also for the other motors studied; see the SI.) Distinctive features are the signals of the aliphatic protons H_a, H_b, and H_c.[12,18] There is only negligible coupling between H_a and H_c due to their relative orientations as a result of the conformation of the five-membered ring, and therefore the doublet at 2.4 ppm can be assigned to H_c. As H_b can couple not only to its geminal proton H_c but also to vicinal proton H_a, the double doublet at 2.9 ppm can be assigned to H_b. The absorption at 3.1 ppm is assigned to proton H_c, which shows a multiplet signal due to the coupling with the methyl group and proton H_b. A solution of stable *trans*-**4** in CD_2Cl_2 was irradiated ($\lambda \geq 365$ nm) at −20 °C, and it was found that all absorptions shifted downfield, indicating the formation of a new isomer which was identified as unstable *cis*-**4** (Figure 2b). Notably, H_c shifts from 2.4 ppm (doublet) to 3.2 ppm (double doublet). Unstable *cis*-**4** adopts a different conformation than that of stable *trans*-**4**, which allows the coupling between H_a and H_c. The new absorption at 3.45 ppm can be identified as H_b, and the multiplet at 3.9 ppm can be assigned as H_a in the unstable *cis* isomer. Extended irradiation resulted in a photostationary state (PSS) with a ratio of 3:2 (unstable *cis*-**4**/stable *trans*-**4**), which was determined by integration of the signals for proton H_c in the stable *trans* and unstable *cis* isomers. Leaving the sample overnight at room temperature with exclusion of light led to the thermal helix inversion from unstable *cis*-**4** to stable *cis*-**4**, which is indicated by a shift of all absorptions (Figure 2c). The doublet at 2.7 ppm was assigned as H_c in the stable *cis* isomer since it has a similar coupling pattern as that in stable *trans* isomer. The absorption at 3.5 ppm shifted downfield and the multiplet at 3.9 ppm shifted upfield, so these absorptions are observed together in the region 3.5−3.7 ppm. Notably, the ratio of stable *cis*-**4**/stable *trans*-**4** (3:2) is equivalent to the ratio of unstable *cis*-**4**/stable *trans*-**4**. It confirms the unidirectionality of the thermal isomerization of unstable *cis*-**4**, indicating the absence of the thermal $E-Z$ isomerization in accordance with our previous observation with related first-generation motors.[12,18] Motors **2**, **3** and **5** also show similar changes in spectra and PSS ratios (unstable *cis*/stable *trans*, 3:2) (SI, Figures S2−S4).

2.4. UV−Vis Spectroscopy Studies. The photochemical isomerization and thermal helix inversion processes of motors **2**−**5** were also studied by UV−vis spectroscopy. The UV−vis spectrum of stable *trans*-**2** in tetrahydrofuran (THF) is shown in Figure 3a (λ_{max} = 355 nm, solid line). The absorption

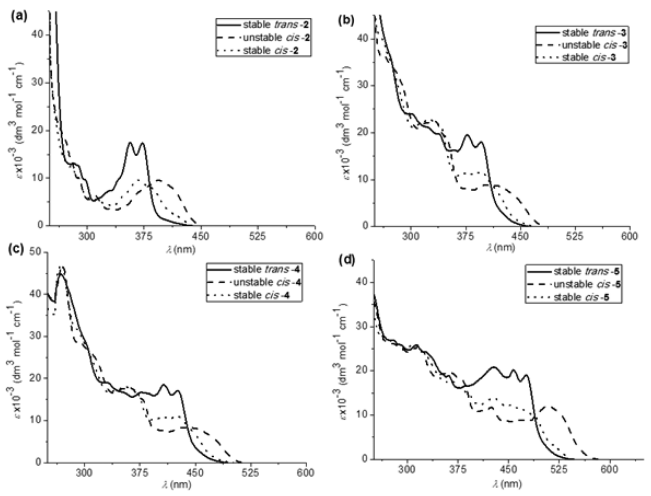

Figure 3. UV−vis spectra in THF of molecular motors, *trans* isomer (solid line), unstable *cis* isomer at PSS (dashed line), and stable *cis* isomer (dotted line) at room temperature: (a) motor **2**, (b) motor **3**, (c) motor **4**, and (d) motor **5**.

maxima at 340 and 355 nm are characteristic absorptions of the stable *trans* isomer of the five-membered first-generation molecular motors.[12] Upon irradiation ($\lambda \geq 365$ nm), a bathochromic shift was observed in the absorption maximum from 355 to 407 nm. The presence of an isosbestic point at 385 nm indicates that no secondary reactions occur during the experiments, and the bathochromic shift can be attributed to the formation of an unstable *cis* isomer (λ_{max} = 407 nm, dashed line, Figure 3a). Subsequently, the sample was left in the dark to allow the thermal helix inversion to occur. A blue shift was observed from 407 to 362 nm, suggesting the generation of stable *cis*-**2** (λ_{max} = 362 nm, dotted line, Figure 3a). Motor **3** was analyzed under identical condition as described above; a clear isosbestic point was found at 412 nm and similar changes (stable *trans*-**3** → unstable *cis*-**3** → stable *cis*-**3**) were observed (Figure 3b), indicating the photochemical and thermal helix inversion processes. Stable *trans*-**4** displayed similar changes in the spectra (Figure 3c) when it was converted to unstable *cis*-**4**

dx.doi.org/10.1021/ja507711h | J. Am. Chem. Soc. 2014, 136, 14924−14932

by irradiation (dashed line) and subsequent to stable *cis*-**4** after warming (dotted line). Besides the featured absorptions of motor at 458 and 472 nm, stable *trans*-**5** shows an additional strong absorption at 420 nm (λ_{max} = 420 nm, solid line, Figure 3d), which can be attributed to the rigid tetramer rod in **5**. After irradiation, the formation of unstable *cis*-**5** generated a bathochromic shift of the long-wavelength absorption band (λ_{max} = 514 nm, dashed line, Figure 3d) and an isosbestic point at 487 nm which is notably red-shifted, compared to those of **3** and **4**. This shift originates from the structure of **5**, as it possesses a more extended conjugated system than **3** and **4**. Leaving the sample in the dark overnight resulted in the formation of stable *cis*-**5** (λ_{max} = 421 nm, dotted line, Figure 3d).

Since the photoisomerization step of molecular motors takes place on the picosecond time scale,[41] the rate of the thermal helix inversion step is rate-limiting in these systems and determines the speed of the motor.[41c,42] The kinetics of the thermal helix inversion step can be studied by UV−vis spectroscopy.[18] The helix inversion, from unstable *cis* to stable *cis* isomer for molecular motors **1**−**5**, was followed by monitoring the UV−vis absorption at a certain wavelength with respect to time at different temperatures (20, 25, 30, and 35 °C; for details, see SI, Figure S5). From these data, the half-life ($t_{1/2}$) and Gibbs free energy of activation ($\Delta^{\ddagger}G°$) at room temperature (20 °C) could be obtained by means of an Eyring analysis (SI, Figure S6), as well as the enthalpy of activation ($\Delta^{\ddagger}H°$) and entropy of activation ($\Delta^{\ddagger}S°$). The kinetic parameters of the thermal helix inversion steps of motors **2**−**5** at room temperature in THF are listed in Table 1.

Table 1. Kinetic Parameters of the Helix Inversion Step of 1−5 in THF at 20 °C

motor	$t_{1/2}$ (min)	$\Delta^{\ddagger}G°$ (kJ/mol)	$\Delta^{\ddagger}S°$ (J/mol·K)	$\Delta^{\ddagger}H°$ (kJ/mol)	calcd $\Delta^{\ddagger}H°$ (kJ/mol)
1	74.0 ± 0.1	93.2	−31.7	84.0	85.9
2	78.5 ± 0.1	93.3	−31.6	84.0	84.5
3	97.8 ± 0.1	93.8	−33.1	84.1	85.2
4	123.7 ± 0.1	94.4	−35.1	84.2	85.0
5	214.6 ± 0.1	95.7	−39.3	84.2	85.6

Motor **2**, which has two flexible hexadecyl chains instead of rigid rods like in **3**−**5**, was found to have almost the same half-life ($t_{1/2}$ = 78.5 min) as parent motor **1** ($t_{1/2}$ = 74.0 min). The $t_{1/2}$ of **3** (97.8 min) is slightly increased compared to that of parent motor **1** by extending the motor core structure with phenylacetylenes on both sides. The $t_{1/2}$ of **4**, which comprises two rigid diphenylacetylene rods attached to the motor, increases to 123.7 min, which indicates that the thermal helix inversion step of motor **4** is almost 2 times slower than that of motor **1**. Motor **5** has the longest rigid rods and exhibits the lowest isomerization rate ($t_{1/2}$ = 214.6 min), which is about 3 times slower than for motor **1**. It suggests that the rate of the thermal helix inversion from unstable *cis* to stable *cis* isomer is affected by the rigidity of the substituent and the length of the rigid substituent. Similar activation enthalpies for **1**−**5** imply that the substituents at the 6- and 6′-positions do not generate any significant steric effects in the fjord region, nor do possible electronic effects influence the thermal helix inversion. These findings are in good agreement with the computationally predicted $\Delta^{\ddagger}H°$ values (SI, Table S3). Therefore, the variation of $\Delta^{\ddagger}G°$ of **1**−**5** is predominately attributed to the change in entropy, $\Delta^{\ddagger}S°$. Increasing $\Delta^{\ddagger}S°$ values of **1**−**5** indicate an increasing demand of order during thermal helix inversion upon an increase in size of the motor. It is postulated that this increase in order is caused by a need to displace solvent molecules during the movement of the motor rods in the thermal helix inversion process from the unstable *cis* isomer to the stable *cis* isomer.[20] This might explain why the half-life of motor **2** remains similar to that of the parent motor, because the flexible hexadecyl alkyl chains can reorientate upon helix inversion to minimize their interactions with solvents, while the rigid substituents cannot. Going from motor **3** to **5**, as the rigid substituents become longer, an increased interaction with the surrounding solvent molecules might be generated, and as a consequence a retardation of the rotary speed is observed. To further exclude the possibility that this increased half-life is due to aggregation of the motors or the rigid substituents, concentration-dependent experiments were performed (Figure 4). The linear relationship between concentration and UV−vis

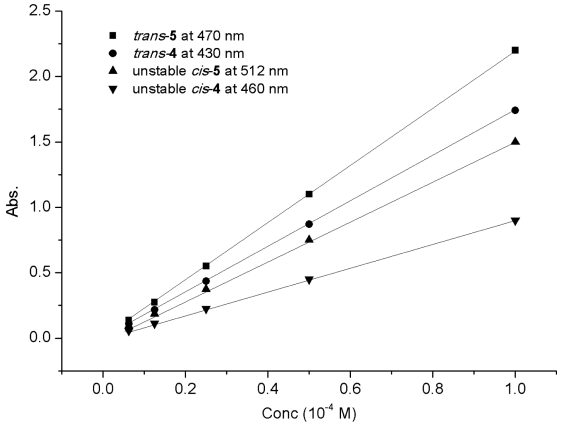

Figure 4. Concentration dependence of the UV−vis absorption of *trans* and *cis* isomers (at PSS) for motors **4** and **5** in THF at room temperature.

absorption for **4** and **5** confirms the absence of aggregation and therefore ensures that the change in $\Delta^{\ddagger}S°$ is attributed to the different interactions between motor and solvent molecules.

2.5. Solvent Effects on Thermal Helix Inversion. To further confirm that different rotary speeds are due to different interactions between motors and solvents, motors **1**−**5** were studied in solvent mixtures of increasing viscosity. Solvent−solvent interactions are higher for a viscous solvent compared to a non-viscous solvent; it is therefore expected that rearrangements of a motor in which it has to displace solvent molecules will be more difficult in solvents of higher viscosity.[20,26] Choosing different solvents of varying viscosities might cause undesired side effects due to nonlinearity in polarity or solubility. In order to keep the changes in motor−solvent interactions linear, a mixed solvent system[25] was chosen in which glycerol was added to THF to a maximum of 80% (volume %). This solvent mixture (η = 1060 cP)[43] is about 2000 times more viscous than THF (η = 0.45 cP). This change in viscosity might affect the rate of thermal helix inversion, but the rate might also be affected by an increase in polarity. Therefore, the rates of thermal helix inversion of motors **1**−**5** were first analyzed in hexane and MeOH, which both possess a viscosity similar to THF but are of lower and higher polarity, respectively.[44] The half-lives of motors **1**−**5** in hexane and

dx.doi.org/10.1021/ja507711h | J. Am. Chem. Soc. 2014, 136, 14924−14932

MeOH are similar to those measured in THF, indicating that the polarity and hydrogen-bonding of a solvent have no significant effect on the thermal helix inversion (SI, Table S1). This suggests that solvent−motor interactions are not dominant a factor, pointing to solvent−solvent interactions, i.e, viscosity, as the origin of retardation (*vide infra*). Concentration dependence was also investigated in THF/glycerol (1/4, v/v) to ensure the absence of aggregation under the experimental conditions (SI, Figure S1). When studied in glycerol/THF (4/1), motors **1**−**5** displayed an increase in half-life of the thermal helix inversion (Figure 5).[45]

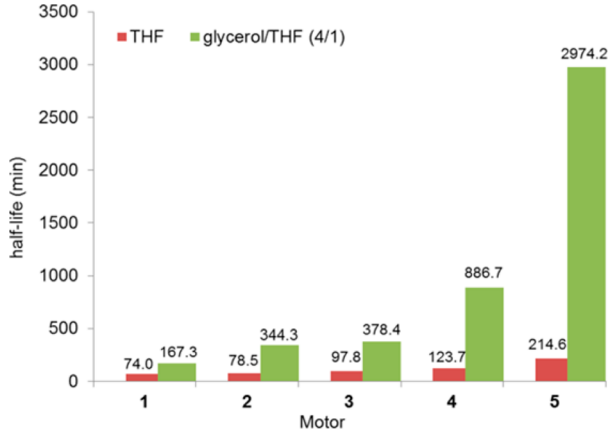

Figure 5. Half-lives of motors **1**−**5** in THF (red) and glycerol/THF (4/1, v/v) (green) at room temperature.

Parent motor **1** ($t_{1/2}$ = 167.3 min) was found to be approximately 2 times slower in glycerol/THF than when measured in THF ($t_{1/2}$ = 74.0 min), whereas motor **5**, which bears two rigid tetramers, showed a prominent retardation of the rotary speed ($t_{1/2}$ = 2974.2 min), being >10 times slower compared to THF ($t_{1/2}$ = 214.6 min). These results confirm that the rotary speed of a motor is affected by the size of its substituents. Notably, the increase in half-life becomes increasingly larger for larger substituents. In THF, motors **3**, **4**, and **5** are 1.3, 1.7, and 2.9 times slower than parent motor **1**, respectively, while motor **2** has almost the same half-life. However, in the viscous solvent mixture, the thermal isomerization steps in the rotary process of motors **2**, **3**, **4**, and **5** are 2.0, 2.3, 5.3, and 17.8 times slower than for motor **1**, respectively. This suggests that the "frictional effect" [22−25,29−33] of the solvent molecules on the motor during the thermal helix inversion becomes more pronounced in viscous solvents.

2.6. Free Volume Model Analysis. To further understand how solvent viscosity and the shape and size of the substituents affect the rotary speed of motors, the *free-volume* model is applied.[46] This model has been used successfully to rationalize the viscosity dependence of processes that involve large-amplitude rotation of molecules.[47−49] According to Doolittle,[46a] molecular motion in a liquid medium is only possible when the free volume (V_f) per molecule is larger than its "critical volume" (V_0). The fluidity (η^{-1}) is proportional to the probability factor $[\exp(-V_0/V_f)]$ for the translation motion. Therefore, the free-volume dependence of the viscosity can be expressed by eq 1, in which A is a proportionality factor.

$$\eta = A \exp(V_0/V_f) \quad (1)$$

In contrast to translation diffusion, molecular rearrangement (such as the thermal helix inversion under investigation) involves only a portion of the molecule. Thus, only a fraction (α) of the critical volume V_0 is required to execute the internal molecular motion. Since α is expressed as a fraction, α is less than 1 because no more than the whole molecule could be subjected to frictional effects during a molecular change; α values higher than 0.3 have been observed before[50] but are rather exceptional.[47−49] The rate constant k of the molecular rearrangement is given by eq 2, and substitution of eq 1 into eq 2 affords eq 3, an expression that was first applied to rationalize the viscosity dependence for the isomerization of stilbene.[47a]

$$k = k^0 \exp(-\alpha V_0/V_f) \quad (2)$$

$$k = k^0 (A/\eta)^\alpha \quad (3)$$

The double-logarithmic form of eq 3 predicts a linear dependence of ln k versus ln η (eq 4). The α value is readily

$$\ln k = \text{const} - \alpha \ln \eta \quad (4)$$

accessible from the slope of the plotted data. For this purpose, motors **1**−**5** were studied in mixed solvent systems of glycerol and THF in different ratios, providing a range of different viscosities (SI).

As is evident from Figure 6, the rate constant k strongly depends on the viscosity for all motors **1**−**5** under

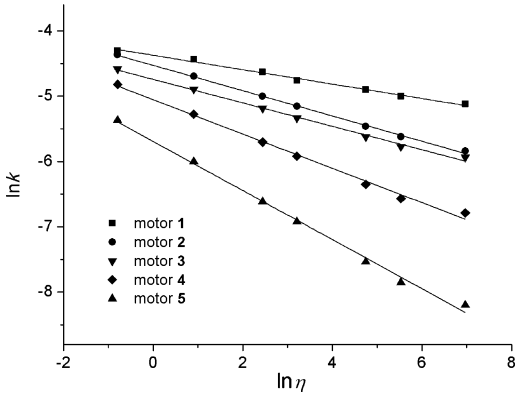

Figure 6. Double-logarithmic plot of solvent viscosity and rate constant of thermal helix inversion of motors **1**−**5**.

investigation, suggesting that the thermal helix inversion of these motors obeys the *free-volume* model over a wide viscosity range. The slope of the double-logarithmic plot affords the α value for each motor (Table 2). The obtained α values are comparable with or exceed the values reported previously for a number of viscosity-controlled isomerizations[47,48] and rearrangements.[49]

As expected, parent motor **1**, which has no substituents (R = H), exhibits the lowest α value, 0.16. The α value for motor **2** with hexadecyl chains was found to be slightly higher, at 0.20. This value is similar to that of motor **3** (α = 0.19), which has phenylacetylene functionalities but is significantly smaller in mass and calculated volume (~2/3) (Table 2). This indicates that the rigidity of the substituents is an important factor affecting the rotary speed of motors. When comparing **2** and **3** to parent motor **1**, it is evident that motor **2** shows a stronger

dx.doi.org/10.1021/ja507711h | J. Am. Chem. Soc. 2014, 136, 14924−14932

Table 2. α Values for Motors 1−5

motor	α	calcd mol volume (Å^3/mol)	$\alpha \times$ mol volume (Å^3/mol)	distance from alkene to center of mass (Å)
1	0.16	441.2	70.60	1.58
2	0.20	1137	227.4	4.78
3	0.19	765.3	145.4	3.71
4	0.28	2837	794.4	9.32
5	0.40	4179	1671	14.1

viscosity dependence than motor **1** or **3**. As mentioned before, motor **2** is almost as fast as its parent analogue **1** in pure THF (Figure 5) since the hexadecyl chains of motor **2** can reorientate to minimize the disruption of the surrounding solvent molecules. However, in viscous solvents these interactions, originating from van der Waals interactions of the long aliphatic chains with glycerol, are not negligible. Therefore, in the most viscous mixture, motor **2** slows down by such a large degree that its speed becomes comparable to that of motor **3** (Figure 5). Going from motor **3** to motors **4** and **5**, the α value increases gradually from 0.19 to 0.28 and 0.40, respectively. It seems to correspond to the hypothesis that substitutions at the 6- and 6′-positions would directly contribute to the rearranging volume ($\alpha \times$ molecular volume, Table 2), since they are on the periphery of the rotating moieties. If the relationship between molecular volume and rearranging volume is linear, an α value of 0.91 would be expected for motor **5** [(volume **5** − volume **1** + rearranging volume **1**)/volume **5** = (4179 − 441.2 + 70.60)/4179)]. However, experimentally a significantly lower value of α = 0.40 is found for motor **5**, which indicates that not all of the added volume also adds to the rearranging volume.

To investigate this phenomenon, intrinsic reaction coordinates (IRCs) of motors **1** and **3** were compared, which showed very similar behaviors of the two motors (Figure 7).

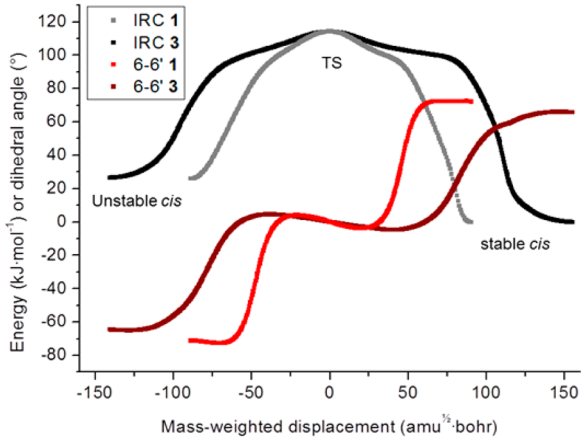

Figure 7. Intrinsic reaction coordinates of thermal helix inversion and 6- and 6′-substituent dihedral angle during thermal helix inversion of motors **1** and **3**.

Motor **3** has to displace a large amount of mass, which is equal to volume on account of a consistent degree of hybrization throughout the molecule (Figure 7). Comparing any internal coordinates during the rotation, for example, the 6- and 6′-substituent dihedral angles plotted in Figure 7, shows the same overall behavior. Since no distinct differences were observed when comparing internal relationships, absolute displacements were analyzed.

An increase in atomic displacement when substituents are added is evident from the IRCs (Figure 7, 179.3 vs 295.6 amu$^{1/2}$·bohr for **1** and **3**, respectively), but the change in ratio between the displacement of the central alkene carbons and the peripheral 6- and 6′-carbons is remarkable (Table 3). This

Table 3. Summed Atomic Displacement of 1 and 3

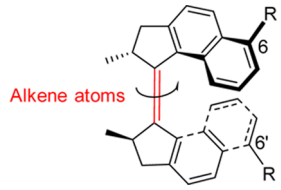

motor	alkene atoms (Å)	atoms 6+6′ (Å)	ratio
1	2.9	8.2	2.8
2	4.0	9.2	2.3

indicates that, even though the internal behavior remains the same (meaning internal coordinates show similar changes during thermal helix inversion), its external behavior (meaning that with respect to the surroundings) changes. The central displacement increases compared to the peripheral movement from motor **1** to **3**. To illustrate this effect, the rotation of the alkene was followed over the course of the IRC (specifically, the angle the double bond makes during the thermal helix inversion with respect to the double bond of the unstable *cis* state, Figure 8).

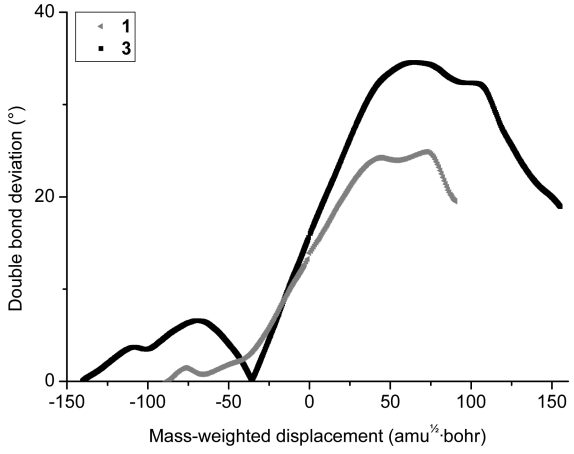

Figure 8. Rotational deviation of the double bond from the unstable *cis* isomer to stable *cis* isomer during thermal helix inversion of **1** and **3**, in degrees.

Figure 8 shows a clear distinction between the rotational behavior of the overcrowded alkene of motors **1** and **3**. The double bond of motor **3** shows not only a larger deviation from its starting point (the unstable *cis* state) but also a change in behavior characterized by the difference in overall shape. This change in behavior is best shown by an overlay of the animations (see Movie 1) of the IRCs of motors **1** (in red) and **3** (in blue). Motors **4** and **5** are expected to follow this behavior, which predicts them to undergo the thermal helix inversion using the same pathway with comparable internal behavior. It is expected that the change in external behavior for motors **4** and **5** will be larger to accommodate for a minimal mass displacement,[51] while still increasing the total amount of

dx.doi.org/10.1021/ja507711h | J. Am. Chem. Soc. 2014, 136, 14924−14932

displacement of mass and, as a consequence, solvent displacement compared to motors **1** and **3** (Table 2). These results explain why the volume added in the 6- and 6′-positions does not add completely to the rearranging volume but only partially because of changes in spatial reorganization. Indeed, motors **4** and **5** possess an increasingly larger volume, which displaces solvent during rotation. The rigid substituents present in motor **5** increase the volume which displaces solvent during rotation from 70.60 Å^3 for parent **1** to 1671 Å^3, thereby using a 24 times larger volume to "stir its surroundings".

3. CONCLUSIONS

A series of first-generation motors with substituents of varying rigidity and length has been synthesized. Their rotation from stable *trans* to stable *cis* isomer upon irradiation and subsequent warming has been confirmed by ^{1}H NMR and UV−vis spectroscopy. The rate of their thermal helix inversion, which is the rate-determining step of the rotary motion of these molecular motors, has been studied in a variety of solvents and solvent mixtures of different polarity and viscosity. The data shows that the size and rigidity of the substituents have a strong effect on the entropic barrier for rotation, decreasing the rate for larger and more rigid substituents. Whereas changes in polarity exhibited no significant influence on the rotation rate, a strong dependency was found for the viscosity of the solvent system. For larger and more rigid substituents, a more pronounced viscosity dependency was found. The *free-volume* model showed that, with increasing substituent size, an increased rearranging volume of the motor participates in the rotation, indicating the requirement for a larger solvent displacement. The rearranging volume of the molecular stirrer has been increased 24-fold from non-substituted motor **1** to tetramer-substituted motor **5**. Computed IRCs show a change in the external rotational behavior upon an increase in substituent size, while the internal relationships remains constant during the thermal helix inversion, explaining the trend found in α values. This work helps us to understand the substituent effect on the rotation of molecular motors and can therefore provide important guidelines for designing more advanced molecules. The results presented here on the thermal isomerization step, being the rate-determining step in the entire rotary process, are in line with medium effects observed very recently on the very fast photochemical isomerization step.[52] The studied viscosity dependence will be important for further application of molecular motors, especially in biosystems and when assembled on surfaces, where environmental effects on molecular motion are expected to play a distinct role.

■ ASSOCIATED CONTENT

Ⓢ Supporting Information

Synthesis and characterization of new compounds; kinetic studies of motors **1**−**5** in different solvents; Eyring plot analyses of motors **2**−**5**; ^{1}H NMR spectra after photochemical and thermal isomerization for **2**, **3**, and **5**; and details on computational studies. This material is available free of charge via the Internet at http://pubs.acs.org.

Ⓦ Web-Enhanced Feature

Movie 1, an animation showing an overlay of the of the IRCs of motors **1** (in red) and **3** (in blue), is available in the HTML version of the paper.

■ AUTHOR INFORMATION

Corresponding Author

b.l.feringa@rug.nl

Notes

The authors declare no competing financial interest.

■ ACKNOWLEDGMENTS

Financial support from NanoNed, The Netherlands Organization for Scientific Research (NWO-CW), the European Research Council (Advanced Investigator Grant, No. 227897 to B.L.F), the Ministry of Education, Culture and Science (Gravity program 024.001.035), and the "Top Research School" program of the Zernike Institute for Advanced Materials under the Bonus Incentive Scheme (BIS) is gratefully acknowledged. The synthesis of compound **2** via organolithium-based cross-coupling method was done with the help of Dr. Martín Fañanás-Mastral.

■ REFERENCES

(1) (a) De Rosier, D. J. *Cell* **1998**, *93*, 17. (b) Kinosita, K.; Yasuda, R.; Noji, H.; Ishiwata, S.; Yoshida, M. *Cell* **1998**, *93*, 21. (c) Boy, P. D. *Nature* **1999**, *402*, 247. (d) Mahadevan, L.; Matsudaira, P. *Science* **2000**, *288*, 95. (e) van den Heuvel, M. G. L.; Dekker, C. *Science* **2007**, *317*, 333. (f) Schliwa, M., Ed. *Molecular Motors*; Wiley-VHC: Weinheim, 2003.

(2) (a) Iwamura, H.; Mislow, K. *Acc. Chem. Res.* **1988**, *21*, 175. (b) Balzani, V.; Gomez-Lopez, M.; Stoddart, J. F. *Acc. Chem. Res.* **1998**, *31*, 405. (c) Stoddart, J. F., Ed. Molecular Machines, Special Issue. *Acc. Chem. Res.* **2001**, *34*, 6. (d) Balzani, V.; Venturi, M.; Credi, A. *Molecular Devices and Machines—A Journey into the Nanoworld*; Wiley-VCH: Weinheim, 2003. (e) Kinbara, K.; Aida, T. *Chem. Rev.* **2005**, *105*, 1377. (f) Browne, W. R.; Feringa, B. L. *Nat. Nanotechnol.* **2006**, *1*, 25. (g) Kay, E. R.; Leigh, D. A.; Zerbetto, F. *Angew. Chem., Int. Ed.* **2007**, *46*, 72. (h) Balzani, V.; Credi, A.; Venturi, M. *Chem. Soc. Rev.* **2009**, *38*, 1542. (i) Coskun, A.; Banaszak, M.; Astumian, R. D.; Stoddart, J. F.; Grzybowski, B. A. *Chem. Soc. Rev.* **2012**, *41*, 19. (j) Feringa, B. L. *J. Org. Chem.* **2007**, *72*, 6635.

(3) Purcell, E. M. *Am. J. Phys.* **1977**, *45*, 3.

(4) (a) Astumian, R. D. *Sci. Am.* **2001**, *285*, 45. (b) Astumian, R. D.; Hanggi, P. *Phys. Today* **2002**, *55*, 33. (c) Astumian, R. D. *Proc. Natl. Acad. Sci. U.S.A.* **2005**, *102*, 1843.

(5) Kottas, G. S.; Clarke, L. I.; Horinek, D.; Michl, J. *Chem. Rev.* **2005**, *105*, 1281.

(6) (a) Kelly, T. R.; De Silva, H.; Silva, R. A. *Nature* **1999**, *401*, 150. (b) Hernandez, J. V.; Kay, E. R.; Leigh, D. A. *Science* **2004**, *306*, 1532. (c) Flectcher, S. P.; Dumur, F.; Pollard, M. M.; Feringa, B. L. *Science* **2005**, *310*, 80.

(7) (a) Bissell, R. A.; Cordova, E.; Kaifer, A. E.; Stoddart, J. F. *Nature* **1994**, *369*, 133. (b) Pease, A. R.; Jeppesen, J. O.; Stoddart, J. F.; Luo, Y.; Collier, C. P.; Heath, J. R. *Acc. Chem. Res.* **2001**, *34*, 433. (c) Ballardini, R.; Balzani, V.; Credi, A.; Gandolfi, M. T.; Venturi, M. *Acc. Chem. Res.* **2001**, *34*, 445. (d) Brouwer, A. M.; Frochot, T.; Gatti, F. G.; Leigh, D. A.; Mottier, L.; Paolucci, F.; Roffia, S.; Wurpel, G. W. H. *Science* **2001**, *291*, 2124. (e) Badjic, J. D.; Balzani, V.; Credi, A.; Silvi, S.; Stoddart, J. F. A. *Science* **2004**, *303*, 1845.

(8) (a) Kline, T. R.; Paxton, W. F.; Mallouk, T. E.; Sen, A. *Angew. Chem., Int. Ed.* **2005**, *44*, 744. (b) Fournier-Bidoz, S.; Arsenault, A. C.; Manners, I.; Ozin, G. A. *Chem. Commun.* **2005**, 441. (c) Ozin, G. A.; Manners, I.; Fournier-Bidoz, S.; Arsenault, A. *Adv. Mater.* **2005**, *17*, 3011. (d) Burdick, J.; Laocharoensuk, R.; Wheat, P. M.; Posner, J.; Wang, J. *J. Am. Chem. Soc.* **2008**, *130*, 8164. (e) Pantarotto, D.; Browne, W. R.; Feringa, B. L. *Chem. Commun.* **2008**, 1533. (e) Stock, C.; Heureux, N.; Wesley, B. R.; Feringa, B. L. *Chem.—Eur. J.* **2008**, *14*, 3146.

(9) von Delius, M.; Geertsema, E. M.; Leigh, D. A. *Nat. Chem.* **2010**, *2*, 96.

(10) (a) Horine, D.; Michl, J. *Proc. Natl. Acad. Sci. U.S.A.* **2005**, *102*, 14175. (b) Berna, J.; Leigh, D. A.; Lubomska, M.; Mendoza, S. M.; Pérez, E. M.; Rudolf, P.; Teobaldi, G.; Zerbetto, F. *Nat. Mater.* **2005**, *4*, 704.
(11) (a) Koumura, N.; Zijlstra, R. W. J.; van Delden, R. A.; Harada, N.; Feringa, B. L. *Nature* **1999**, *401*, 152. (b) Koumura, N.; Geertsema, E. M.; van Gelder, M. B.; Meetsma, A.; Feringa, B. L. *J. Am. Chem. Soc.* **2002**, *124*, 5037.
(12) ter Wiel, M. K. J.; van Delden, R. A.; Meetsma, A.; Feringa, B. L. *J. Am. Chem. Soc.* **2003**, *125*, 15076.
(13) Ruangsupapichat, N.; Pollard, M. M.; Harutyunyan, S. R.; Feringa, B. L. *Nat. Chem.* **2011**, *3*, 53.
(14) (a) Irie, M., Ed. Photochroism: Memories and Switches, Special Issue. *Chem. Rev.* **2000**, *100*, 5. (b) Feringa, B. L., Ed. *Molecular Switches*; Wiley-VCH: Weinheim, 2001.
(15) van Delden, R. A.; Koumura, N.; Harada, N.; Feringa, B. L. *Proc. Natl. Acad. Sci. U.S.A.* **2002**, *99*, 4945.
(16) Wang, J.; Kulago, A.; Browne, W. R.; Feringa, B. L. *J. Am. Chem. Soc.* **2010**, *132*, 4191.
(17) Wang, J.; Hou, L.; Browne, W. R.; Feringa, B. L. *J. Am. Chem. Soc.* **2011**, *133*, 8162.
(18) Lubbe, A. S.; Ruangsupapichat, N.; Caroli, G.; Feringa, B. L. *J. Org. Chem.* **2011**, *76*, 8599.
(19) Wang, J.; Feringa, B. L. *Science* **2011**, *331*, 1429.
(20) Klok, M.; Janssen, L. P. B. M.; Browne, R. W.; Feringa, B. L. *Faraday Discuss.* **2009**, *143*, 319.
(21) (a) Forster, T.; Hoffman, G. *Z. Phys. Chem. N. F.* **1971**, *75*, 63. (b) Griffiths, J. *Chem. Soc. Rev.* **1972**, *1*, 481. (c) Rothenberger, G.; Negus, D. K.; Hochstrasser, R. M. *J. Chem. Phys.* **1983**, *79*, 5360. (d) Courtney, S. H.; Fleming, G. R. *J. Chem. Phys.* **1985**, *83*, 215. (e) Doering, W. v. E.; Birladeanu, L.; Cheng, X. H.; Kitagawa, T.; Sarma, K. *J. Am. Chem. Soc.* **1991**, *113*, 4558. (f) Zeglinski, D. M.; Waldeck, D. H. *J. Phys. Chem.* **1988**, *92*, 692. (g) Liao, L.; Stellacci, F.; McGrath, D. V. *J. Am. Chem. Soc.* **2004**, *126*, 2181.
(22) (a) Sung, C. S. P.; Lamarre, L.; Tse, M. K. *J. Am. Chem. Soc.* **1979**, *13*, 666. (b) Eisenbach, C. D. *Polymer* **1980**, *21*, 1176. (c) Gille, K.; Knoll, H.; Quitzsch, K. *Int. J. Chem. Kinet.* **1999**, *31*, 337. (d) Serra, F.; Terentjev, E. M. *Macromolecules* **2008**, *41*, 981.
(23) (a) Malkin, S.; Fischer, E. *J. Phys. Chem.* **1964**, *68*, 1153. (b) Velsko, S. P.; Waldeck, D. H.; Fleming, G. R. *J. Chem. Phys.* **1983**, *78*, 249. (c) Lee, M.; Bain, A. J.; McCarthy, P. J.; Han, C. H.; Haseltine, J. N.; Smith, A. B.; Hochstrasser, R. M. *J. Chem. Phys.* **1986**, *85*, 4341. (d) Courtney, S. H.; Kim, S. K.; Cononica, S.; Fleming, G. R. *J. Chem. Soc., Faraday Trans. 2* **1986**, *82*, 2065. (e) Zeglinski, D. M.; Waldeck, D. H. *J. Phys. Chem.* **1988**, *92*, 692. (f) Mohrschladta, R.; Schroeder, J.; Schwarzer, D.; Troe, J.; Vohringer, P. *J. Chem. Phys.* **1994**, *101*, 7566.
(24) (a) Adam, W.; Diedering, M.; Trofimov, A. V. *J. Am. Chem. Soc.* **2002**, *124*, 5427. (b) Adam, W.; Librera, C.; Trofimov, A. V. *J. Am. Chem. Soc.* **2002**, *124*, 11936.
(25) (a) Scarlata, S.; Rholam, M.; Weber, G. *Biochemistry* **1984**, *23*, 6789. (b) Rholam, M.; Scarlata, S.; Weber, G. *Biochemistry* **1984**, *23*, 6793.
(26) Hutchison, J. A.; Uji-I, H.; Deres, A.; Vosch, T.; Rocha, S.; Müller, S.; Bastian, A. A.; Enderlein, J.; Nourouzi, H.; Li, C.; Herrmann, A.; Müllen, K.; De Schryver, F.; Hofkens, J. *Nat. Nanotechnol.* **2014**, *9*, 131.
(27) Mal, N. K.; Fujiwara, M.; Tanaka, Y. *Nature* **2003**, *421*, 350.
(28) Grebel-Koehler, D.; Liu, D.; De Feyter, S.; Enkelmann, V.; Weil, T.; Engels, C.; Samyn, C.; Müllen, K.; De Schryver, F. C. *Macromolecules* **2003**, *36*, 578.
(29) (a) Velsko, S. P.; Fleming, G. R. *J. Chem. Phys.* **1982**, *76*, 3553. (b) Mohrschladt, R.; Schroeder, J.; Schwarzer, D.; Troe, J.; Vohringer, P. *J. Chem. Phys.* **1994**, *101*, 7566.
(30) Onganer, Y.; Yin, M.; Bessire, D. R.; Quitevis, E. L. *J. Phys. Chem.* **1993**, *97*, 2344.
(31) Benniston, A. C.; Harriman, A. *J. Chem. Soc., Faraday Trans.* **1994**, *90*, 2627.
(32) Laia, C.; Costa, S. *Chem. Phys. Lett.* **2002**, *354*, 435.
(33) Gulam, R. M.; Takahashi, T.; Ohga, Y. *Phys. Chem. Chem. Phys.* **2009**, *11*, 5170.
(34) Adam, W.; Trofimov, A. V. *Acc. Chem. Res.* **2003**, *36*, 571.
(35) Pollard, M. M.; Wesenhagen, P. V.; Pijper, D.; Feringa, B. L. *Org. Biomol. Chem.* **2008**, *6*, 1605.
(36) Ziener, U.; Godt, A. *J. Org. Chem.* **1997**, *62*, 6137.
(37) Vicario, J.; Meetsma, A.; Feringa, B. L. *Chem. Commun.* **2005**, 5910.
(38) Wielopolski, M.; Atienza, C.; Clark, T.; Guldi, D. M.; Martin, N. *Chem.—Eur. J.* **2008**, *14*, 6379.
(39) Giannerini, M.; Fañanás-Mastral, M.; Feringa, B. L. *Nat. Chem.* **2013**, *5*, 667.
(40) Mori, A.; Kawashima, J.; Shimada, T.; Suguro, M.; Hirabayashi, K.; Nishihara, Y. *Org. Lett.* **2000**, *2*, 2935.
(41) (a) Schuddeboom, W.; Jonker, S. A.; Warman, J. M.; de Haas, M. P.; Vermeulen, M. J. W.; Jager, W. F.; de Lange, B.; Feringa, B. L.; Fessenden, R. W. *J. Am. Chem. Soc.* **1993**, *115*, 3286. (b) Zijlstra, R. W. J.; van Duijnen, P. T.; Feringa, B. L.; Steffen, T.; Duppen, K.; Wiersma, D. A. *J. Phys. Chem. A* **1997**, *101*, 9828. (c) Augulis, R.; Klok, M.; Feringa, B. L.; van Loosdrecht, P. H. M. *Phys. Stat. Sol. C* **2009**, *6*, 181. (d) Conyard, J.; Addison, K.; Heisler, I. A.; Cnossen, A.; Browne, W. R.; Feringa, B. L.; Meech, S. R. *Nat. Chem.* **2012**, *4*, 547.
(42) (a) Feringa, B. L.; Koumura, N.; Van Delden, R. A.; ter Wiel, M. K. J. *Appl. Phys. A: Mater. Sci. Process.* **2002**, *75*, 301. (b) Klok, M.; Browne, W. R.; Feringa, B. L. *Phys. Chem. Chem. Phys.* **2009**, *11*, 9124. (c) Geertsema, E. M.; van der Molenb, S. J.; Martensc, M.; Feringa, B. L. *Proc. Natl. Acad. Sci. U.S.A.* **2009**, *106*, 16919.
(43) Dynamic viscosity is measured by using the glass capillary viscometer at 20 °C.
(44) Reichardt, C.; Welton, T. *Solvents and Solvent Effects in Organic Chemistry*; Wiley-VCH: Weinheim, Germany, 2010.
(45) Similar trends were observed in DCM, DMF, and DMF/glycerol; see SI, Table S2.
(46) (a) Doolittle, A. K. *J. Appl. Phys.* **1951**, *22*, 1471. (b) Cohen, M. *J. Chem. Phys.* **1959**, *31*, 1164.
(47) (a) Gegiou, D.; Muszkat, K. A.; Fisher, E. *J. Am. Chem. Soc.* **1968**, *90*, 12. (b) Forster, T.; Hoffman, G. *Z. Phys. Chem. N. F.* **1971**, *75*, 63. (c) Tredwell, C. J.; Osborne, A. D. *J. Chem. Soc., Faraday Trans. 2* **1980**, *76*, 1627.
(48) (a) Velsko, S. P.; Fleming, G. R. *J. Chem. Phys.* **1982**, *76*, 3553. (b) Velsko, S. P.; Waldeck, D. H.; Fleming, G. R. *J. Chem. Phys.* **1983**, *78*, 249. (c) Keery, K. M.; Fleming, G. R. *Chem. Phys. Lett.* **1982**, *93*, 322. (d) Bagchi, B.; Oxtoby, D. *J. Chem. Phys.* **1983**, *78*, 2735.
(49) (a) Adam, W.; Grune, M.; Diedering, M.; Trofimov, A. V. *J. Am. Chem. Soc.* **2001**, *123*, 7109. (b) Adam, W.; Marti, V.; Sahin, C.; Trofimov, A. V. *Chem. Phys. Lett.* **2001**, *340*, 26.
(50) (a) Waldeck, D. H. *Chem. Rev.* **1991**, *91*, 415. (b) Onganer, Y.; Yin, M.; Bessire, D. R.; Quitevis, E. L. *J. Phys. Chem.* **1993**, *97*, 2344. (c) Asano, T. *Pure Appl. Chem.* **1999**, *71*, 1691. (d) Jin, H.; Liang, M.; Arzhantsev, S.; Li, X.; Maroncelli, M. *J. Phys. Chem. B* **2010**, *114*, 7565.
(51) IRCs of **4** and **5** are computationally too demanding.
(52) Conyard, J.; Cnossen, A.; Browne, W. R.; Feringa, B. L.; Meech, S. R. *J. Am. Chem. Soc.* **2014**, *136*, 9692.